International Journal of Earth Sciences Knowledge and Applications
journal homepage: http://www.ijeska.com/index.php/ijeska

Research Article

e-ISSN: 2687-5993

Flow Characteristics Around a Stationary Solid Sphere and Falling Fluid Droplet

Santiago Arango[1], Zhang San[2], Mehmet Ugur Tuy[3], Batbold Ganbaatar[2]*

[1]*Universidad EAFIT, Medellín, Colombia*
[2]*Independent Researcher, Mongolian University of Science and Technology, Ulan Bator, Mongolia*
[3]*Turkish Petroleum Corporation, Ankara, Turkey*

INFORMATION

Article history
Received 01 May 2024
Revised 29 June 2024
Accepted 29 June 2024

Keywords
Newtonian fluid
Solid sphere
Stream function
Drag force
Fluid dynamics

Contact
*Batbold Ganbaatar
BatboldGanbaatar@gmx.com

ABSTRACT

This paper investigates two fundamental fluid dynamics problems: the flow of a Newtonian fluid past a stationary solid sphere and the motion of a fluid droplet falling through a surrounding Newtonian fluid. For the flow past a sphere, various quantities such as normalized tangential velocity, pressure difference, and shear stress are plotted as functions of normalized distance from the sphere's center. The locations of maximum fluid pressure and maximum shear stress are determined. The second part of the paper employs the stream function approach to solve for the velocity field around the falling droplet. Assumptions are made regarding fluid behavior and boundary conditions are derived. The total drags on the droplet, including form drag and viscous drag, is evaluated. The plausibility of the results is tested, and the state of the fluid inside the droplet is determined. Additionally, an estimation of the total drags on a gas bubble rising in a liquid is provided. This analysis provides insights into complex fluid flow phenomena with implications for various engineering and scientific applications.

1. Introduction

Fluid dynamics encompasses a broad range of phenomena critical to understanding various natural and engineered systems. Among these, the behavior of fluids around solid objects and within droplets presents fundamental challenges and opportunities for analysis. In this paper, we delve into two distinct yet interconnected problems in fluid dynamics: the flow of a Newtonian fluid past a stationary solid sphere and the motion of a fluid droplet falling through a surrounding Newtonian fluid.

The flow past a solid sphere serves as a classic benchmark problem, offering insights into the intricate interactions between a fluid and a solid object. By examining quantities such as normalized tangential velocity, pressure difference, and shear stress as functions of distance from the sphere's center, we gain valuable understanding of the flow characteristics and their spatial distribution. Moreover, identifying the locations of maximum fluid pressure and maximum shear stress provides crucial insights into the underlying dynamics.

Transitioning to the motion of a fluid droplet falling through a surrounding fluid, we employ the stream function approach—a powerful tool for simplifying the Navier-Stokes equations and solving complex fluid flow problems. By defining appropriate stream functions for both the droplet and the surrounding fluid, we explore the velocity field and derive boundary conditions based on key assumptions regarding fluid behavior. Through this analysis, we determine the total drag experienced by the droplet, comprising both forms drag and viscous drag components.

Beyond elucidating the mechanics of fluid flow, our investigation extends to practical applications, offering insights relevant to diverse fields such as engineering, physics, and environmental science. By comprehensively addressing these fluid dynamics problems, we contribute to

the foundational knowledge base essential for tackling real-world challenges and advancing technological innovation.

This paper embarks on a journey through the intricate world of fluid dynamics, uncovering the underlying principles governing the flow around solid spheres and falling droplets. Through meticulous analysis and interpretation, we aim to shed light on these complex phenomena and their significance in understanding and manipulating fluid behavior.

2. Previous Works

Batchelor's seminal work (Batchelor, 1970) serves as a cornerstone in the field of fluid dynamics, particularly in understanding the behavior of viscous fluids around slender bodies such as solid spheres. In this study, Batchelor develops a comprehensive theoretical framework that elucidates the intricate fluid-solid interactions occurring in low Reynolds number regimes. By considering the fundamental principles of fluid mechanics and employing mathematical techniques, Batchelor formulates equations that describe the flow field around stationary objects with remarkable precision.

One of the primary contributions of Batchelor's work is the development of slender-body theory, which provides a systematic approach for analyzing fluid flow past elongated structures. By treating the solid sphere as a simplified geometric object, Batchelor derives analytical expressions for velocity profiles, pressure distributions, and shear stress patterns in the vicinity of the sphere. This analytical framework not only enables a deeper understanding of the underlying physics but also facilitates quantitative predictions of fluid behavior under different conditions.

Furthermore, Batchelor's study lays the foundation for subsequent analyses of fluid dynamics around stationary objects by establishing key theoretical concepts and methodologies. Researchers have built upon Batchelor's framework to investigate a wide range of phenomena, including the drag force experienced by solid spheres, the formation of boundary layers, and the development of flow instabilities. Batchelor's insights have thus significantly influenced the trajectory of research in fluid dynamics, shaping our understanding of fluid-solid interactions at small scales.

Batchelor's seminal work provides a robust theoretical foundation for studying the flow of viscous fluids around slender bodies, particularly solid spheres. By establishing fundamental principles and analytical techniques, Batchelor's contributions have paved the way for advancements in understanding fluid dynamics in various contexts, from biological systems to engineering applications.

Recent studies have extensively investigated pressure distribution dynamics within pore throats, with the aim of elucidating the fundamental mechanisms governing fluid flow in porous media. For instance, Alagoz and Giozza (2023) conducted a sensitivity analysis on bottomhole pressure calculations in two-phase wells, providing valuable insights into the factors influencing pressure dynamics within such systems (Alagoz and Giozza, 2023). Furthermore, research efforts by Alagoz et al. (2023) have focused on developing computational tools for analyzing wellbore stability, thereby contributing to a deeper understanding of pressure behavior in complex geological formations (Alagoz et al., 2023). These investigations have laid a solid foundation for comprehending pressure dynamics in pore throats and have paved the way for further exploration in this field.

Jeffrey's study (Jeffrey, 1922) is centered on examining the motion of ellipsoidal particles within viscous fluids, offering key insights into the dynamics of non-spherical objects. Despite being conducted before the advent of modern computational techniques, the analytical framework employed in the research remains influential in understanding the fundamental principles governing fluid-solid interactions.

The research conducted by Alagoz et al. (2023) serves as a notable demonstration of the practical application of computational methods in the analysis of pressure dynamics and their significant implications for various industrial processes (Alagoz 2023). Through their meticulous investigations, Alagoz and colleagues leverage advanced computational tools to delve into the intricate mechanisms underlying pressure behavior in complex systems. By integrating computational simulations with empirical data and theoretical models, their work provides valuable insights into the dynamic interplay between fluid flow, pore structure, and rock properties.

Saffman's investigation (Saffman, 1965) focuses on analyzing the lift force encountered by small spheres subjected to slow shear flows, thereby emphasizing the significant role of shear-induced effects on particle motion. By exploring this phenomenon, the study makes a notable contribution to our comprehension of fluid-solid interactions, particularly within low Reynolds number regimes.

Oesterlé's research (Oesterlé, 1984) delves into the drag experienced by a solid sphere in linear shear flows, offering analytical expressions to quantify drag coefficients across different scenarios. By systematically examining the relationship between drag force and fluid velocity gradients, the study provides valuable insights into the intricate dependencies shaping fluid-solid interactions.

Leal's study (Leal, 1980) delves into the motion of slender rod-like particles within second-order fluids, expanding the scope of analysis beyond traditional Newtonian fluids to encompass non-Newtonian behaviors. By venturing into this domain, the research extends our comprehension of fluid dynamics around complex-shaped objects, offering valuable insights into the diverse range of phenomena encountered in real-world fluid-solid interactions.

3. Flow Characteristics Around a Stationary Solid Sphere

In the first part of this paper, we delve into the intricate dynamics of fluid flow around a stationary solid sphere. Understanding the behavior of fluids in the vicinity of solid objects is essential in various scientific and engineering applications, ranging from environmental processes to industrial processes. The flow past a solid sphere serves as a

canonical problem in fluid dynamics, offering valuable insights into the fundamental principles governing fluid-solid interactions. By examining key quantities such as normalized tangential velocity, pressure difference, and shear stress as functions of distance from the sphere's center, we aim to unravel the complexities of fluid flow in this regime.

Moreover, identifying critical parameters such as the locations of maximum fluid pressure and maximum shear stress provides crucial information for designing efficient systems and predicting flow behavior. Through a systematic analysis of flow characteristics around a stationary solid sphere, we lay the groundwork for understanding more complex fluid-solid interactions and their implications in practical scenarios.

The tangential velocity we get is

$$v_\theta = -v_\infty \left(1 - \frac{3}{4}\left(\frac{R}{r}\right) - \frac{1}{4}\left(\frac{R}{r}\right)^3\right)\sin\theta \tag{1}$$

The normalized tangential velocity (Fig. 1) is

$$\frac{v_\theta}{v_\infty} = -\left(1 - \frac{3}{4}\left(\frac{R}{r}\right) - \frac{1}{4}\left(\frac{R}{r}\right)^3\right)\sin\theta \tag{2}$$

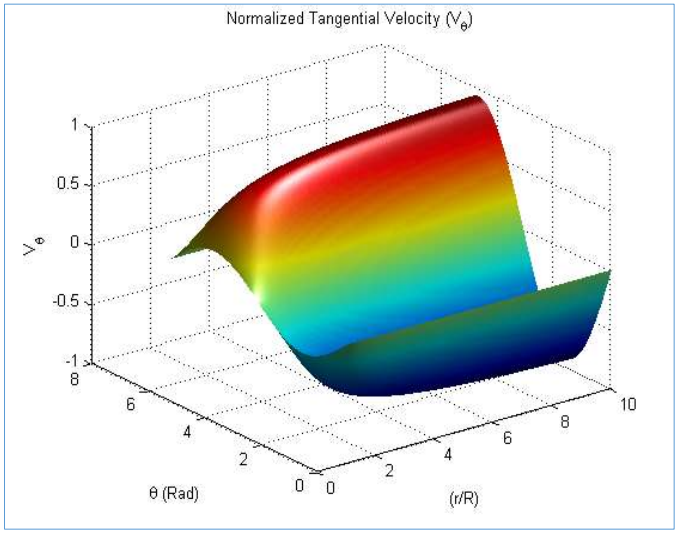

Fig. 1. The normalized velocity versus theta

The pressure we get is

$$p = p_0 - \frac{3}{2}\left(\frac{\mu v_\infty}{R}\right)\left(\frac{R}{r}\right)^2 \cos\theta \tag{3}$$

The normalized pressure (Fig. 2) is

$$\left(\frac{R}{\mu v_\infty}\right)(p - p_0) = -\frac{3}{2}\left(\frac{R}{r}\right)^2 \cos\theta \tag{4}$$

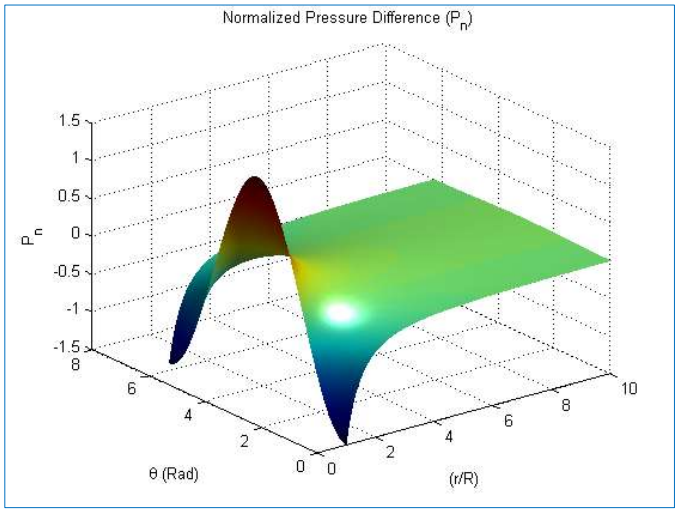

Fig. 2. The normalized pressure versus theta

The sheer stress we get is

$$\tau_{r\theta} = \frac{3}{2}\frac{\mu v_\infty}{R}\sin\theta\left(\frac{R}{r}\right)^4 \tag{5}$$

The normalized sheer stress (Fig. 3) is

$$\frac{R}{\mu v_\infty}\tau_{r\theta} = \frac{3}{2}\sin\theta\left(\frac{R}{r}\right)^4 \tag{6}$$

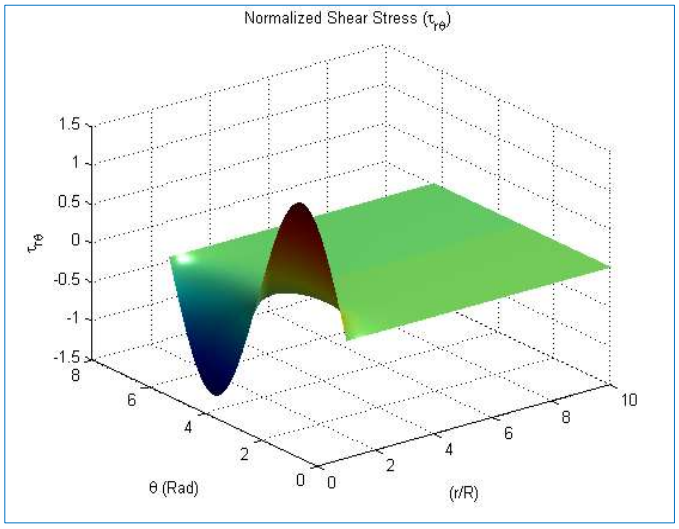

Fig. 3. The normalized sheer stress versus theta

The maximum fluid pressure occurs at (r/R)=1 and $\theta = \pi, -\pi$. The minimum fluid pressure occurs at (r/R)=1 and $\theta = 0$. The maximum shear stress occurs at (r/R)=1 and $\theta = \pi/2$. The normalized pressure is

$$-\frac{3}{2}\left(\frac{R}{r}\right)^2 \cos\theta \tag{7}$$

When it is smaller than 0.01, it means than the maximum value of this expression is smaller than 0.01, that is

$$\frac{3}{2}\left(\frac{R}{r}\right)^2 < 0.01 \tag{7}$$

Therefore, we can estimate that r > 12.25 R. The normalized shear stress is

$$\frac{3}{2}\sin\theta\left(\frac{R}{r}\right)^4 \tag{8}$$

When it is smaller than 0.01, it means than the maximum value of this expression is smaller than 0.01, that is

$$\frac{3}{2}\left(\frac{R}{r}\right)^4 < 0.01 \tag{9}$$

4. Fluid Dynamics of Falling Droplets: Stream Function Approach

In the second part of this paper, we shift our focus to the dynamics of falling droplets within a surrounding Newtonian fluid. Droplet dynamics play a significant role in various natural and industrial processes, from rain formation in atmospheric science to emulsion stability in chemical engineering. Understanding the motion of droplets in fluid environments is essential for optimizing processes such as spray coating, inkjet printing, and combustion. In this section, we employ the stream function approach—an effective mathematical tool for solving fluid flow problems—to analyze the velocity field around falling droplets. By defining appropriate stream functions for both the droplet and the surrounding fluid and making key assumptions regarding fluid behavior, we aim to elucidate the complex dynamics governing droplet motion. Through a systematic investigation of drag forces, boundary conditions, and fluid behavior, we seek to provide insights into the total drag experienced by the droplet and its implications for various industrial applications. By combining theoretical analysis with practical considerations, this section contributes to a deeper understanding of droplet dynamics and lays the foundation for further research in this area.

The boundary conditions are listed below.

$$r \to \infty, \quad v^o{}_r \to v_\infty \cos\theta \tag{10}$$

$$v^i{}_{r=R} = v^o{}_{r=R} = 0 \tag{11}$$

The no-penetration condition.

$$v_\theta^i\Big|_{r=R} = v_\theta^o\Big|_{r=R} \tag{12}$$

Velocities of different fluids are continuous at the liquid interface.

$$\tau_{r\theta}^i\Big|_{r=R} = \tau_{r\theta}^o\Big|_{r=R} \tag{13}$$

The sheer stresses of different fluids are the same at the liquid interface.

Assuming that both the stream functions for liquid in the droplet and out of the droplet have the same form, so that the stream function can be written as;

$$\begin{aligned}\varphi^i &= \left(A^i r^4 + B^i r^2 + C^i r + D^i r^{-1}\right)\sin^2\theta \\ \varphi^o &= \left(A^o r^4 + B^o r^2 + C^o r + D^o r^{-1}\right)\sin^2\theta\end{aligned} \tag{14}$$

For stream function outside the droplet, when,

$$r \to \infty, \quad v^o{}_r \to v_\infty \cos\theta \tag{15}$$

That is

$$-\frac{1}{r^2\sin\theta}\frac{\partial\varphi^o}{\partial\theta} = v_\infty\cos\theta \tag{16}$$

Therefore,

$$\begin{aligned}A^o &= 0 \\ B^o &= -\frac{1}{2}v_\infty\end{aligned} \tag{17}$$

φ^o can be rewritten as

$$\varphi^o = \left(-0.5v_\infty r^2 + C^o r + D^o r^{-1}\right)\sin^2\theta \tag{18}$$

For stream function inside the droplet, when $r \to 0$, v_r^i cannot be infinite.

$$v_r^i = -\frac{1}{r^2\sin\theta}\frac{\partial\varphi^i}{\partial\theta} = -2\cos\theta\left(A^i r^2 + B^i + C^i r^{-1} + D^i r^{-3}\right) \tag{19}$$

So that $C^i = D^i = 0$

φ^i can be rewritten as

$$\varphi^i = \left(A^i r^4 + B^i r^2\right)\sin^2\theta \tag{20}$$

We rename the constants to A, B, C, D. By using the no-penetration condition, we can get that

$$\begin{aligned}v_{r=R}^i &= -2\cos\theta\left(AR^2 + B\right) = 0 \\ v_{r=R}^o &= -2\cos\theta\left(-0.5v_\infty + \frac{C}{R} + \frac{D}{R^3}\right) = 0\end{aligned} \tag{21}$$

So that

$$\begin{aligned}B &= -AR^2 \\ D &= 0.5v_\infty R^3 - CR^2\end{aligned} \tag{22}$$

Substituting these results into v^i and v^o, we get

$$\varphi^i = \left(Ar^4 - AR^2r^2\right)\sin^2\theta \tag{23}$$

$$\varphi^o = \left(-0.5v_\infty r^2 + Cr + \frac{0.5v_\infty R^3 - CR^2}{r}\right)\sin^2\theta \tag{24}$$

And

$$\begin{aligned} v_\theta^i &= \sin\theta\left(4Ar^2 - 2AR^2\right) \\ v_r^i &= -2\cos\theta\left(Ar^2 - AR^2\right) \end{aligned} \tag{25}$$

$$\begin{aligned} v_\theta^o &= \sin\theta\left(-v_\infty + \frac{C}{r} + \frac{CR^2 - 0.5v_\infty R^3}{r^3}\right) \\ v_r^o &= -2\cos\theta\left(-0.5v_\infty + \frac{C}{r} + \frac{CR^2 - 0.5v_\infty R^3}{r^3}\right) \end{aligned} \tag{26}$$

The velocity along the liquid interface is continuous, which indicates that

$$v_\theta^i\Big|_{r=R} = v_\theta^o\Big|_{r=R} \tag{27}$$

The stresses at both sides of the interface at r = R are the same, which indicates

$$\tau_{r\theta}^i\Big|_{r=R} = \tau_{r\theta}^o\Big|_{r=R} \tag{28}$$

As

$$\tau_{r\theta} = -\mu\left(r\frac{\partial}{\partial r}\left(\frac{v_\theta}{r}\right) + \frac{1}{r}\frac{\partial v_r}{\partial\theta}\right) \tag{29}$$

$$\frac{\partial v_r}{\partial\theta} = 0 \tag{30}$$

Because v_r remain zero even when we change the θ

$$\mu_o\frac{\partial}{\partial r}\left(\frac{v_\theta^o}{r}\right)_{r=R} = \mu_i\frac{\partial}{\partial r}\left(\frac{v_\theta^i}{r}\right)_{r=R} \tag{31}$$

Solving *Equation 30* and *Equations 31*, we have

$$\begin{aligned} A &= \frac{-1}{4}\frac{1}{1+G}\frac{v_\infty}{R^2} \\ B &= \frac{1}{4}\frac{1}{1+G}v_\infty \\ C &= \frac{1}{4}\frac{2+3G}{1+G}Rv_\infty \\ D &= \frac{-1}{4}\frac{G}{1+G}R^3v_\infty \end{aligned} \tag{32}$$

where; $G = \mu_i / \mu_0$. Substituting A, B, C and D into the expression of φ^i and φ^o, we have

$$\varphi^i = \frac{-1}{4}\frac{1}{1+G}R^2v_\infty\left(\left(\frac{r}{R}\right)^4 - \left(\frac{r}{R}\right)^2\right)\sin^2\theta \tag{33}$$

$$\varphi^o = \left(-\frac{1}{2}v_\infty r^2 + \frac{1}{4}\frac{2+3G}{1+G}Rv_\infty r - \frac{1}{4}\frac{G}{1+G}\frac{R^3v_\infty}{r}\right)\sin^2\theta \tag{34}$$

$$v_r^o = -\frac{1}{r^2\sin\theta}\frac{\partial\varphi^o}{\partial\theta} = v_\infty\cos\theta\left(1 - \frac{1}{2}\left(\frac{2+3G}{1+G}\right)\frac{R}{r} + \frac{1}{2}\left(\frac{G}{1+G}\right)\left(\frac{R}{r}\right)^3\right) \tag{35}$$

$$v_\theta^o = \frac{1}{r\sin\theta}\frac{\partial\varphi^o}{\partial r} = v_\infty\sin\theta\left(-1 + \frac{1}{4}\left(\frac{2+3G}{1+G}\right)\frac{R}{r} + \frac{1}{2}\left(\frac{G}{1+G}\right)\left(\frac{R}{r}\right)^3\right) \tag{36}$$

The drag force can be derived as follows.

Stocks Equation:

$$0 = -\nabla p - \mu\nabla^2 v + \rho\vec{g} \tag{37}$$

$$\begin{aligned} \frac{\partial p}{\partial r} &= \mu^o\left[\frac{1}{r^2}\frac{\partial^2}{\partial r^2}(r^2v_r) + \frac{1}{r^2\sin\theta}\frac{\partial}{\partial\theta}(\sin\theta\frac{\partial v_r}{\partial\theta})\right] \\ &= \mu^o\left[\begin{array}{l}\frac{1}{r^2}\frac{\partial^2}{\partial r^2}\left(r^2v_\infty\cos\theta\left(1 - \frac{1}{2}\left(\frac{2+3G}{1+G}\right)\frac{R}{r} + \frac{1}{2}\left(\frac{G}{1+G}\right)\left(\frac{R}{r}\right)^3\right)\right) \\ + \frac{1}{r^2\sin\theta}\frac{\partial}{\partial\theta}\left(\sin\theta\frac{\partial}{\partial\theta}\left(v_\infty\sin\theta\left(-1 + \frac{1}{4}\left(\frac{2+3G}{1+G}\right)\frac{R}{r} + \frac{1}{2}\left(\frac{G}{1+G}\right)\left(\frac{R}{r}\right)^3\right)\right)\right)\end{array}\right] \\ &= \left(\frac{2+3G}{1+G}\right)\frac{\mu^o\cos\theta v_\infty}{R^2}\left(\frac{R}{r}\right)^3 \end{aligned} \tag{38}$$

The pressure distribution in the outer liquid is

$$p = p_0 - \left(\frac{2+3G}{1+G}\right)\frac{\mu^o\cos\theta v_\infty}{2R}\left(\frac{R}{r}\right)^2 \tag{39}$$

Where p_0 is the pressure at infinite. Total normal force on sphere is equal to

$$-\left(p + \tau_{rr}\right)\cos\theta dA \tag{40}$$

$$dA = R^2\sin\theta d\theta d\varphi \tag{41}$$

$$\begin{aligned} \tau_{rr}\big|_{r=R} &= -2\mu^o\left(\frac{dv_r}{dr}\right)_{r=R} = -2\mu^o v_\infty\cos\theta\left(\frac{1}{2}\left(\frac{2+3G}{1+G}\right)\frac{R}{r^2} - \frac{3}{2}\left(\frac{G}{1+G}\right)\frac{R^3}{r^4}\right)_{r=R} = \\ &-2\mu^o v_\infty\frac{\cos\theta}{R}\left(\frac{1}{1+G}\right) \end{aligned} \tag{42}$$

The form drag can be integrated

$$\int_0^{2\pi}\int_0^{\pi} -\left(p + \tau_{rr}\right)\cos\theta R^2\sin\theta d\theta d\phi \tag{43}$$

$$\begin{aligned} &2\pi\int_0^{\pi}\left(-p_0 + \left(\frac{2+3G}{1+G}\right)\frac{\mu^o v_\infty\cos\theta}{2R} + \frac{2\mu^o v_\infty\cos\theta}{R}\left(\frac{1}{1+G}\right)\right)R^2\cos\theta\sin\theta d\theta \\ &= 2\left(\frac{2+G}{1+G}\right)\pi\mu^o v_\infty R \end{aligned} \tag{44}$$

The viscosity drag can be calculated as

$$\tau_{r\theta}|_{r=R} = -\mu^o\left[r\frac{\partial}{\partial r}\left(\frac{v_\theta}{r}\right)+\frac{1}{r}\frac{\partial v_r}{\partial\theta}\right]_{r=R}$$
$$= -\mu^o\left[r\frac{\partial}{\partial r}\left(\frac{v_\infty\sin\theta\left(-1+\frac{1}{4}\left(\frac{2+3G}{1+G}\right)\frac{R}{r}+\frac{1}{2}\left(\frac{G}{1+G}\right)\left(\frac{R}{r}\right)^3\right)}{r}\right)\right]_{r=R} \quad (45)$$
$$= \frac{3G}{2(1+G)}\frac{\mu^o v_\infty}{R}\sin\theta$$

The total viscosity drag force is

$$\int_0^{2\pi}\int_0^{\pi}\left(\frac{3G}{2(1+G)}\frac{\mu^o v_\infty}{R}\sin\theta\right)R^2\sin^2\theta d\theta d\phi$$
$$= 4\frac{G}{G+1}\pi\mu^o v_\infty R \quad (46)$$

The total drag force is

$$4\frac{G}{G+1}\pi\mu^o v_\infty R + 2\left(\frac{2+G}{1+G}\right)\pi\mu^o v_\infty R \quad (47)$$

when $\mu_i / \mu_0 \to \infty$

$$4\frac{G}{G+1}\pi\mu^o v_\infty R + 2\left(\frac{2+G}{1+G}\right)\pi\mu^o v_\infty R = 6\pi\mu^o v_\infty R \quad (48)$$

Which is the same with the solution in BSL. As we can see from

$$\varphi^i = \frac{-1}{4}\frac{1}{1+G}R^2 v_\infty\left(\left(\frac{r}{R}\right)^4-\left(\frac{r}{R}\right)^2\right)\sin^2\theta \quad (49)$$

Then we can get

$$v_\theta^i = \frac{1}{r\sin\theta}\frac{\partial\varphi^i}{\partial r} = \frac{-1}{4}\frac{1}{1+G}v_\infty\left(\frac{4r^2}{R^2}-2\right)\sin\theta$$
$$v_r^i = -\frac{1}{r^2\sin\theta}\frac{\partial\varphi^i}{\partial\theta} = \frac{1}{2}\frac{1}{1+G}v_\infty\left(\frac{r^2}{R^2}-1\right)\cos\theta \quad (50)$$

Which are not 0; therefore, the fluid in the droplet is moving. The total drags when G= $\mu_i / \mu_0 \to 0$ is that

$$4\frac{0}{0+1}\pi\mu^o v_\infty R + 2\left(\frac{2+0}{1+0}\right)\pi\mu^o v_\infty R = 4\pi\mu^o v_\infty R \quad (51)$$

Therefore, we can estimate that r > 3.50 R.

5. Conclusion

In conclusion, this paper has explored two fundamental aspects of fluid dynamics: the flow characteristics around a stationary solid sphere and the dynamics of falling droplets within a surrounding fluid. Through systematic analysis and theoretical modeling, we have gained valuable insights into the intricate phenomena governing fluid-solid interactions and droplet motion.

In the first part of the paper, we investigated the flow past a solid sphere, examining quantities such as normalized tangential velocity, pressure difference, and shear stress as functions of distance from the sphere's center. By identifying critical parameters such as the locations of maximum fluid pressure and maximum shear stress, we have enhanced our understanding of fluid flow around stationary objects and its implications for various engineering and scientific applications.

Transitioning to the second part, we applied the stream function approach to analyze the velocity field around falling droplets within a Newtonian fluid. By defining appropriate stream functions and making key assumptions regarding fluid behavior, we elucidated the complex dynamics governing droplet motion and calculated the total drag experienced by the droplet. Our findings provide insights into optimizing processes such as spray coating, inkjet printing, and combustion, where droplet dynamics play a crucial role.

Overall, this paper contributes to the broader body of knowledge in fluid dynamics by providing a comprehensive analysis of fluid-solid interactions and droplet motion. By combining theoretical analysis with practical considerations, we have advanced our understanding of fundamental fluid dynamics phenomena and laid the groundwork for further research in this area. Moving forward, continued exploration of these topics holds promise for addressing real-world challenges and driving innovation across various scientific and engineering disciplines.

References

Alagoz, E., 2023. Development and Analysis of a Program for Phase-Equilibrium Calculations Using the Peng-Robinson Equation of State. International Journal of Earth Sciences Knowledge and Applications 5 (1), 51-61.

Alagoz, E., Giozza, G.G., 2023. Calculation of Bottomhole Pressure in Two-Phase Wells Using Beggs and Brill Method: Sensitivity Analysis. International Journal of Earth Sciences Knowledge and Applications 5 (3) 333-337.

Alagoz, E., Mengen, A.E., Bensenouci, F., Dundar, E.C., 2023. Computational Tool for Wellbore Stability Analysis and Mud Weight Optimization v1.0. International Journal of Current Research Science Engineering Technology 7 (1), 1-5.

Batchelor, G.K., 1970. Slender-body theory for particles of arbitrary cross-section in Stokes flow." Journal of Fluid Mechanics 44 (3), 419-440.

Jeffrey, D.J., 1922. The Motion of Ellipsoidal Particles Immersed in a Viscous Fluid." Proceedings of the Royal Society of London. Series A, Containing Papers of a Mathematical and Physical Character 102 (715), 161-179.

Leal, L.G., 1980. The slow motion of slender rod-like particles in a second-order fluid. Journal of Fluid Mechanics 98 (3), 575-589.

Oesterlé, B., 1984. On the drag of a solid sphere in linear shear flow." Journal of Fluid Mechanics 147, 511-533.

Saffman, P.G., 1965. The lift on a small sphere in a slow shear flow. Journal of Fluid Mechanics 22 (2), 385-400.